

## The Cavity Method for the Rigidity Transition

J. Barré,<sup>1</sup> A. R. Bishop,<sup>1</sup> T. Lookman<sup>1</sup>, and A. Saxena<sup>1</sup>

*Received September 3, 2004; accepted November 23, 2004*

---

In order to motivate an analogy between the rigidity theory and combinatorial optimization, we have used the cavity method to study the floppy to rigid transition in a 2-dimensional (2D) random graph as well as in a 3D small world chain. Our analytic results are in excellent agreement with numerical studies using the pebble game algorithm. We also illustrate that a transfer matrix method is equivalent to the cavity method at the replica symmetric level.

---

**KEY WORDS:** Rigidity transition; combinatorial optimization; cavity method.

### 1. INTRODUCTION

The rigidity problem dates back at least to the 19th century, when Maxwell made a decisive contribution. The problem can be presented as follows. Consider an ensemble of atoms, which can *a priori* move freely in the plane, or in 3D space; these atoms are linked by a certain number of rigid bonds. One would like to know if the resulting network is rigid or floppy, that is, can it bear an applied stress or not? It is clear that when there are too few bonds, the network is floppy, and will continuously deform without energy cost under stress; as bonds are added, it becomes rigid: this is the rigidity transition. Rigidity theory has been very successfully applied to the study of network glasses,<sup>(1-3)</sup> and has also recently been used to analyze proteins.<sup>(4)</sup>

Although the rigidity problem is physically clear, analytic approaches are difficult and few. Maxwell introduced a mean-field like approach, which consists of counting the number of degrees of freedom of the system and the number of constraints induced by the bonds. The transition is

---

<sup>1</sup>Theoretical Division, Los Alamos National Laboratory, Los Alamos, NM 87545, USA; e-mail: jbarre@cns.lanl.gov

estimated to take place when these two numbers are equal. Critical exponents were estimated by renormalization group analysis.<sup>(5)</sup> To our knowledge, exact solutions have been obtained only for Random Bond Models, which have no finite size loops in the thermodynamic limit, thus allowing for the use of Cayley tree techniques. Duxbury *et al.* and Chubinsky *et al.* solved several types of Random Bond Models using a transfer matrix method.<sup>(6–8)</sup>

The rigidity problem bears striking similarities with a number of combinatorial problems. We briefly introduce one of them, K-SAT. An instance of the K-SAT problem involves  $N$  Boolean variables  $x_i \in \{0, 1\}$ , and  $M$  constraints. The constraints take the form of “OR” functions of  $K$  variables, for instance  $x_1$  OR  $\bar{x}_3$  OR  $x_9$ , if  $K = 3$  ( $\bar{x}_3$  means NOT  $x_3$ ). The instance is said to be satisfiable if there exists an assignment of the variables  $x_i$  such that all the constraints are satisfied, and unsatisfiable otherwise. The problem is to know whether a given instance is satisfiable or not, and the answer obviously depends on the ratio  $M/N$  (constraints/variables). The analogy with the rigidity problem is easy to draw: Boolean variables correspond to the atoms and their degrees of freedom; logical constraints to the physical constraints imposed by the bonds; a satisfiable instance of K-SAT to a floppy network; an unsatisfiable instance to a rigid one; and finally the control parameter  $M/N$  to the average number of bonds per atom. Recently, important analytical breakthroughs have been made for K-SAT and other combinatorial problems using a method borrowed from spin glass theory, termed the cavity method.<sup>(9)</sup> It is then interesting to ask if the cavity method can help to solve rigidity models. It turns out that this cavity method is essentially equivalent to the transfer matrix one developed in refs. 6–8 for the rigidity problem.

The similarity between K-SAT and the rigidity problem has been recognized in the literature, as cross-citations from articles in both fields testify.<sup>(10,11)</sup> It seems, however, that the analogy has not been developed in depth: the goal of this paper is to provide a firmer foundation, by demonstrating clearly the link between the transfer matrix method and the cavity method. This will bring the analogy to an operational stage, where ideas and methods can be transferred from one field to the other. In particular, the concept of an “intermediate phase” as a precursor to the transition recently emerged in both fields;<sup>(9,12)</sup> we will discuss the possible similarity between them. Also, different conjectures have been made for combinatorial problems concerning the link between a phase transition and the onset of computational complexity. We will assess where the rigidity problem stands in this respect. Finally, we present a solution for the rigidity transition of a small world network using the cavity method.

The plan of the paper is as follows. In Section 2, we present the graph theoretic approach to rigidity, which underlies the analogy with combinatorial problems. In Section 3, we apply the cavity method to solve a 2D rigidity model. In Section 4, we study the rigidity transition of a “small world” chain, embedded in 3D space. In Section 5, we discuss the results and what we learn from the analogy with combinatorial problems.

## 2. GRAPH THEORY AND RIGIDITY

Graph theoretic approaches to rigidity were initiated by Laman in the 1970's.<sup>(13)</sup> They were developed during the last decade, leading to powerful algorithms for the analysis of the rigidity of a network.<sup>(14-16)</sup> To represent the problem as a graph theoretic one is a first step in using the cavity method.

Let us consider a network embedded in 2 dimensions so that each atom has *a priori* 2 degrees of freedom. We first consider the case where the edges impose bond stretching constraints only, so that each edge corresponds to one constraint. Each edge removes a degree of freedom of one of the adjacent vertices; this is represented by the orientation of the edge. After an orientation has been assigned to each edge, the number of degrees of freedom of a vertex is two minus the number of incoming bonds. A negative number of degrees of freedom means that the vertex is stressed.

The number of “floppy modes”, or remaining degrees of freedom, is given by

$$H = \sum_{i=1}^N \max(d_i, 0), \quad (1)$$

where  $d_i$  is the (possibly negative) number of degrees of freedom of vertex  $i$ . Figure 1 shows examples of graph orientations and number of floppy modes. The actual number of floppy modes of the network is  $H_0$  computed by minimizing  $H$  over all the configurations of the system, that is over all possible orientations of the edges. The problem is now reduced to a ground state calculation. If the network does not have finite size loops in the thermodynamic limit, the cavity method at zero temperature is well suited for this purpose. Unlike the example of Fig. 1, however, this procedure does not always give the exact number of floppy modes of the network; nevertheless, the difference is negligible for large random networks. We see that adding an edge reduces  $H_0$  by at most 1; if an edge does not reduce  $H_0$ , we call it a redundant bond.

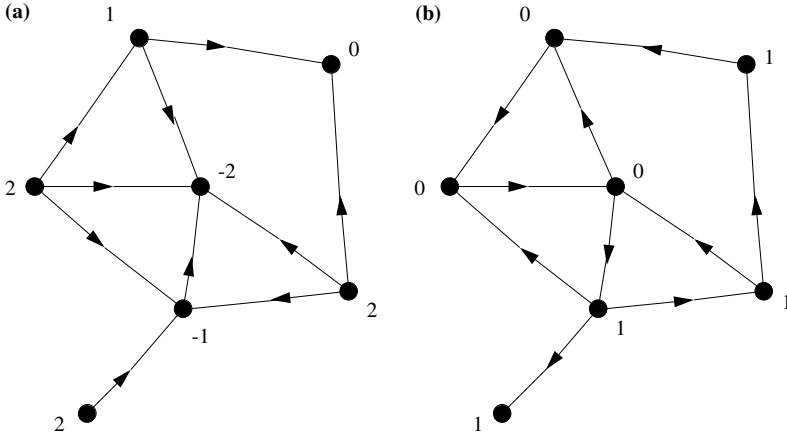


Fig. 1. An example of a graph with two orientations. (a) is not optimal and corresponds to  $H=7$ . (b) is optimal, and corresponds to  $H=4$ . Note that the actual number of degrees of freedom of the graph is indeed 4: two global translations, one global rotation, and the rotation of the 1-fold coordinated site around its neighboring site.

It is possible to consider bond-bending constraints as well, i.e. not only the lengths of the bonds but also the angles between two adjacent bonds are considered as constraints. It is known that 3D bond-bending networks are equivalent to “body-bar” networks, in which vertices have 6 degrees of freedom, and each edge represents 5 constraints.<sup>(16)</sup> One can then repeat the construction above. To define a configuration, the orientation of the edges is not sufficient any more, and one must now choose how each edge partitions its 5 constraints between the two adjacent vertices. Solutions of random bond models with bond-bending constraints are obtained using this idea in ref. 7.

We now have a graph description of the problem to solve. We are ready to implement the general cavity formalism at zero temperature (i.e. we are interested here in the ground state). We refer the reader to ref. 17 for the different steps of the cavity method, where it is clearly explained. In the following, we emphasize the details specific to the rigidity model.

### 3. RIGIDITY OF A 2D RANDOM GRAPH

As an application, we first apply the cavity method to a random graph embedded in 2D space defined as follows: each site is connected randomly to 6 neighbors; each bond is then kept with probability  $p$  and removed with probability  $1-p$ . Each bond carries a bond stretching

constraint only. The network is floppy for  $p$  small, and rigid for  $p$  close to 1. This model has been studied and solved with the transfer matrix method in ref. 6. The solution given here is fully equivalent and serves as an illustration for the cavity method.

One first defines the cavity sites as sites with only five neighbors (or rather potential neighbors, each bond being effectively present with probability  $p$ ). One then assigns a field  $h$  to each cavity site, such that  $h=1$  if the site has one or two degrees of freedom left, and  $h=0$  if the site has no degree of freedom left. At the simplest level, which corresponds to a replica symmetry hypothesis,<sup>(17)</sup> the cavity method describes the system by  $P(h)$ , the probability that a vertex has the field  $h$ . This probability distribution is computed as follows. Construct a new cavity site by adding one site, picking five existing cavity sites and joining them to the new site with probability  $p$ , see Fig. 2. If the graph is large enough, the fields  $\{h_i\}_{i=1}^5$  of the five old cavity sites are independent and distributed according to  $P(h)$ . From the value of the fields  $\{h_i\}_{i=1}^5$ , one computes  $h_0$ , the field at the new cavity site, which must be distributed according to  $P(h)$ . This procedure thus leads to a self-consistent equation for the distribution  $P$ , see Table I.

Let  $p_0$  and  $p_1$  be the probabilities for a cavity field to be equal to 0 and 1, respectively. Collecting the contributions from Table I, one obtains the equation:

$$\begin{aligned}
 p_0 = & 10p^2(1-p)^3 p_0^2 + 10p^3(1-p)^2(p_0^3 + 3p_0^2 p_1) \\
 & + 5p^4(1-p)(p_0^4 + 4p_0^3 p_1 + 6p_0^2 p_1^2) \\
 & + p^5(p_0^5 + 5p_0^4 p_1 + 10p_0^3 p_1^2 + 10p_0^2 p_1^3).
 \end{aligned}
 \tag{2}$$

$p_0=0$  is always a solution of Eq. (2). This is the only one at low  $p$ . Two new solutions appear for  $p > p^*$ , one of which is unstable. This same equation was obtained for a Cayley tree in a slightly different manner in ref. 6. As in usual first order phase transitions, the transition does not take

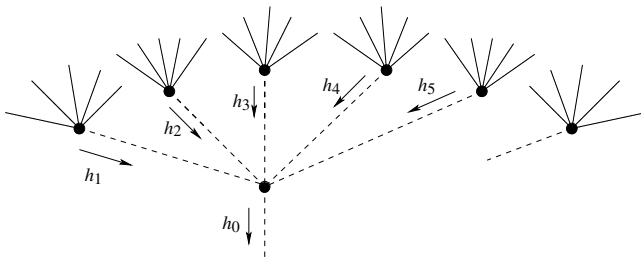


Fig. 2. Adding a new cavity site. Each bond is effectively present with a probability  $p$ .

**Table I. Table to Obtain the Self-consistent Equation for  $P(h)$**

neighb.	prob.	$h_i$	$h_0$
0	$(1-p)^5$	–	1
1	$5p(1-p)^4$	0, 1	1
2	$10p^2(1-p)^3$	(00)	0
		(01), (11)	1
3	$10p^3(1-p)^2$	(000), (001)	0
		(011), (111)	1
4	$5p^4(1-p)$	(0000), (0001), (0011)	0
		(0111), (1111)	1
5	$p^5$	(00000), (00001), (00011), (00111)	0
		(01111), (11111)	1

First column: number of neighbors of the new cavity site; second: probability to have this number of neighbors; third: incoming fields  $h_i$ ; fourth: resulting outgoing field  $h_0$ . The basic rule is as follows: each link with a neighbor which carries a field  $h_i = 0$  can be oriented toward the new cavity site; at least two neighbors with  $h_i = 0$  are thus necessary and sufficient to have  $h_0 = 0$ .

place at  $p^*$ . In ref. 6, the authors locate the transition through a type of Maxwell construction; the cavity method offers another natural possibility, through a direct computation of the number of floppy modes per site, as explained in the following.

Once the distribution  $P(h)$  (that is  $p_0$  and  $p_1$ ) is known, one can compute the ground state energy, or the number of floppy modes in the system. Consider a graph  $G_{N,N_c}$  with  $N$  sites and  $N_c$  cavity sites, with  $1 \ll N_c \ll N$ . Then the ground state energy of  $G_{N,N_c}$  can be written as  $E_{N,N_c} = NE_0 + N_c E_c$ ,<sup>(17)</sup> where  $E_c$  is the mean energy of the cavity sites. We want to compute  $E_0$ , the energy per site for a graph without any cavity site. Figures 3 and 4 show the operations of site addition and link addition on a graph  $G_{N,N_c}$ . Adding a site shifts the energy by  $\Delta E_1$ , and transforms  $G_{N,N_c}$  to  $G_{N+1,N_c-6}$ . Thus  $\Delta E_1 = E_0 - 6E_c$ . Similarly, adding a link shifts the energy by  $\Delta E_2$  and transforms  $G_{N,N_c}$  to  $G_{N,N_c-2}$ . Thus  $\Delta E_2 = -2E_c$ . Finally, one deduces the expression for  $E_0$ :

$$E_0 = \Delta E_1 - 3\Delta E_2. \tag{3}$$

$\Delta E_1$  and  $\Delta E_2$  can be calculated when the distribution  $P(h)$  is known, by constructing a table like Table II. When adding a new site, one picks up six cavity sites and links each one of them to the new site with probability  $p$ ; the new sites thus has  $k$  neighbors, with  $0 \leq k \leq 6$ . This operation adds one site, thus 2 degrees of freedom, and  $k$  links, which remove

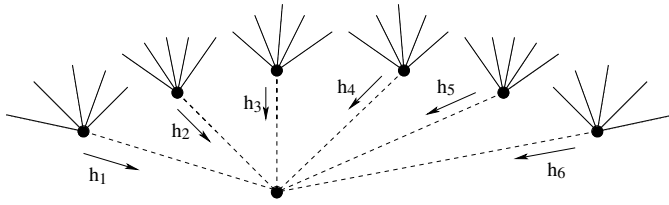


Fig. 3. Adding a new site.

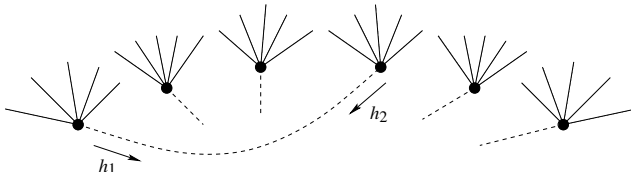


Fig. 4. Adding a new link between two cavity sites.

Table II. Table to Calculate  $\Delta E_1$

neighb.	prob.	$h_i$	$\Delta E_1$
0	$(1-p)^6$	—	+2
1	$6p(1-p)^5$	0, 1	+1
2	$15p^2(1-p)^4$	(00), (01), (11)	0
3	$20p^3(1-p)^3$	(000)	0
		(001), (011), (111)	-1
4	$15p^4(1-p)^2$	(0000)	0
		(0001)	-1
		(0011), (0111), (1111)	-2
5	$6p^5(1-p)$	(00000)	0
		(00001)	-1
		(00011)	-2
		(00111), (01111), (11111)	-3
6	$p^6$	(000000)	0
		(000001)	-1
		(000011)	-2
		(000111)	-3
		(001111), (011111), (111111)	-4

First column: number of neighbors of the newly added site; second: probability to have this number of neighbors; third: incoming fields  $h_i$ ; fourth: resulting  $\Delta E_1$ .

$k$  degrees of freedom minus the number of redundant bonds. This number of redundant bonds depends on the cavity fields  $h_1, \dots, h_k$ . Table II summarizes and details these arguments, allowing the calculation of  $\Delta E_1$ .

Table III. Table to Calculate  $\Delta E_2$ 

$(h_1, h_2)$	prob.	$\Delta E_2$
(00)	$p_0^2$	0
(01), (11)	$2p_0p_1 + p_1^2$	-1

First column: cavity fields  $h_1, h_2$  of the newly linked sites; second: probability to have these cavity fields; third: resulting  $\Delta E_2$ .

When adding a new bond, one removes a degree of freedom (thus  $\Delta E_2 = -1$ ) unless the two cavity sites linked by the new bond both carry a field  $h=0$ ; in this case, there is no available degree of freedom to remove and  $\Delta E_2=0$ . This is summarized in Table III and the equation:

$$\Delta E_2 = -(p_1^2 + 2p_0p_1). \quad (4)$$

Collecting the contributions of Table II for  $\Delta E_1$  and using Eq. (4) for  $\Delta E_2$ , one computes the number of floppy modes per site  $E_0$  from Eq. (3).  $E_0$  along the branch of solution  $p_0=0$  can be calculated exactly, and is given by  $E_0^{(1)} = 2 - 3p$ ; since the number of links per site is precisely  $3p$ , this corresponds to a graph with no redundant link: each bond reduces by 1 the number of degrees of freedom. This is the only solution at low  $p$ . At larger  $p$ , a non-trivial solution appears, the energy of which  $E_0^{(2)}$  has to be computed numerically; when it crosses the straight line  $E_0^{(1)}$ , it becomes stable: this is the rigidity transition, see Fig. 5. The transition probability is estimated to be  $p_c \simeq 0.656$ ; this coincides of course with the transfer matrix results.<sup>(6)</sup>

This concludes the solution of this 6-connected graph by the cavity method. Although this is equivalent to the transfer matrix solution of ref. 6, the cavity calculation emphasizes the precise formal link with spin glass theory and combinatorial problems such as K-SAT. In the next section, we give another example of the application of the cavity method to a more complicated model: a small world chain.

#### 4. RIGIDITY OF A SMALL WORLD CHAIN

The solution of the previous model was facilitated by the fact that the graph had no local structure, the bonding being independent of the physical position of the vertex. This situation may make sense for some combinatorial optimization problems with no underlying physical space, but is



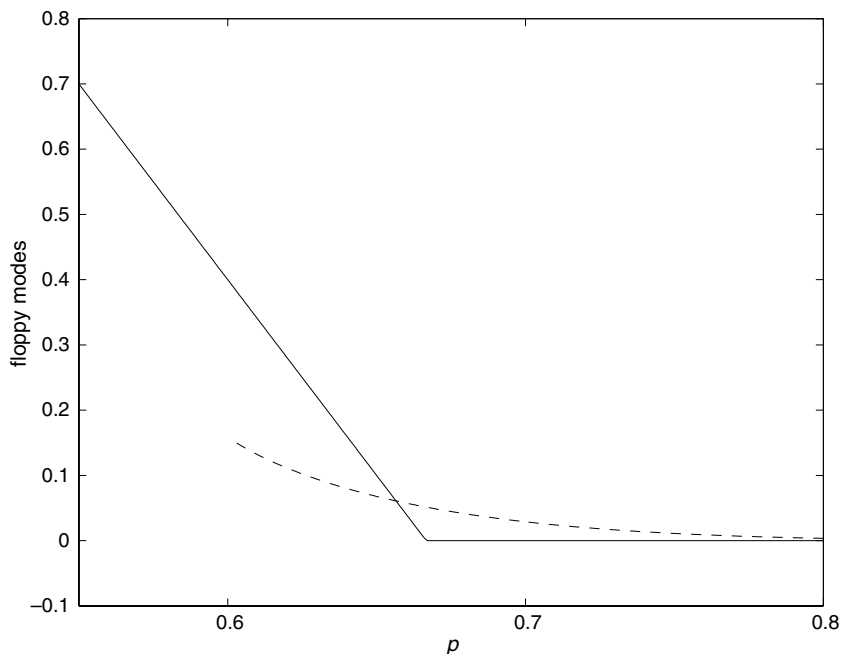


Fig. 5. Number of floppy modes per site as a function of the probability  $p$ . The solid straight line is the low  $p$  solution; the dashed line is the non-trivial solution. The intersection gives  $p_c \simeq 0.656$ . The straight line  $E_0^{(1)} = 2 - 3p$  is replaced by  $E_0^{(1)} = 0$  for  $p > 2/3$  since a negative number of degrees of freedom makes no physical sense.

usually a drastic approximation in physical situations. The cavity method is unlikely to be able to handle realistic situations for the rigidity transitions, where loops with a finite number of sites are allowed. However, it can solve models with some local structure. We give here the example of a chain of sites embedded in 3D space, for which the lengths of the bonds as well as the angles between them are fixed (i.e. bond-stretching and bond-bending constraints). In addition to the bonds forming the chain, a certain number of bonds connecting randomly two sites, called “small world bonds”, are added. This can be considered as a simple model of a macromolecule folded onto itself, so that some sites far from one another along the chain are effectively bonded; see Fig. 6. Small world networks were introduced some years ago<sup>(18)</sup> in an attempt to study more realistic models of real networks than the usual regular lattices and Erdős–Renyi random graphs. They have since then been the subject of intense study; this, however, to our knowledge is the first time they are studied in the context of the rigidity transition.

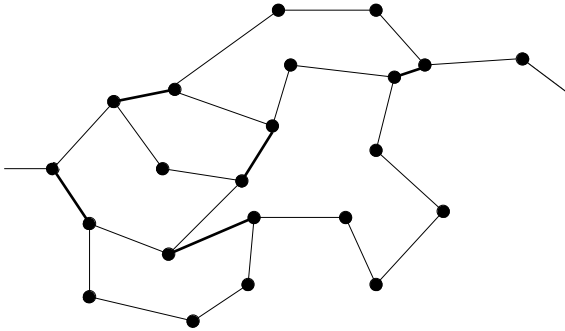


Fig. 6. An example of a “small world chain”. The small world links superimposed on the 1D structure are highlighted with bold lines.

To be precise, the “small world” bonds are added to the chain as follows: the  $N$  sites are matched in  $N/2$  pairs, and a bond is placed between each pair with a probability  $p$ . Thus each site is part of at most one small world bond.<sup>2</sup> For  $p=0$ , the network is a simple chain, floppy: all dihedral rotations along the chain are allowed. For  $p=1$ , the network is rigid. As explained above, if the bond angles as well as the bond lengths are considered as constraints, we have to use a graph representation where the number of degrees of freedom per site is 6, and each bond can freeze 5 degrees of freedom.

We call cavity sites those sites that lack one bond. There are two types of cavity sites: type 1 if the missing bond is a chain bond, type 2 if the missing bond is a small world bond. Thus, there are also two types of fields, called generically  $g$  and  $h$ , associated to cavity sites of type 1 and 2, respectively. The fields  $g$  and  $h$  can now take any value from 0 (if no degree of freedom is left to the site) to 5 (if 5 or 6 degrees of freedom are left to the site).

Figure 7 shows the addition of type 1 and type 2 cavity sites. From this figure, one obtains the consistency equations for the probability distributions  $P_g$  and  $P_h$  of the fields  $g$  and  $h$ , as was done for the 6-connected random graph previously. As above, the only solution at low  $p$  is  $P_g(g=5)=1$ ,  $P_h(h=5)=1$ , that is a floppy chain. At higher  $p$ , a new solution appears, corresponding to a rigid chain (a third one is again unstable). One must evaluate the energy of the new solution to locate the phase transition. This is done as before, computing first the energy shifts  $\Delta E_2^C$  when adding a chain bond (Fig. 8a),  $\Delta E_2^{SW}$  when adding a small world bond

<sup>2</sup>The more usual case where an Erdős–Rényi random graph is superimposed on the chain could be solved as well.

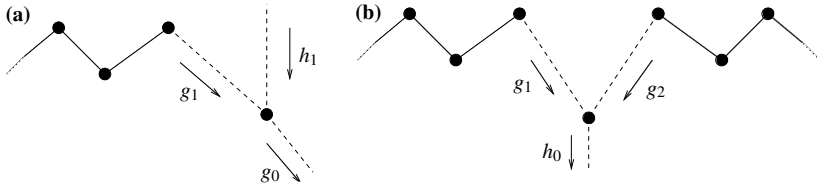


Fig. 7. In the left panel, a site is added to a half chain, receiving from it the field  $g_1$ , and connected with probability  $p$  to another site via a small world link, receiving from it the field  $h_1$ .  $g_0$ , the outgoing field, is calculated as a function of  $g_1$ ,  $h_1$  and  $p$ . In the right panel, a site is connecting two half chains, receiving from them the fields  $g_1$  and  $g_2$ , which generate an outgoing field  $h_0$ . From these two figures are generated the two equations allowing the calculation of  $P_g$  and  $P_h$ .

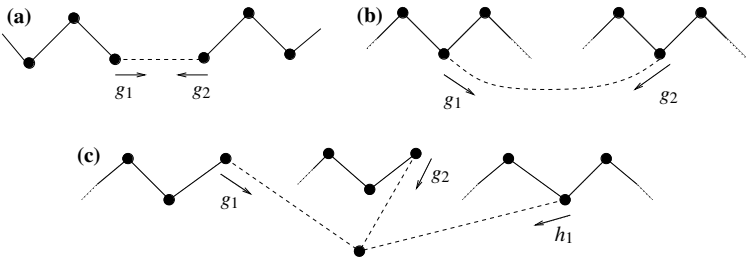


Fig. 8. Panel (a): addition of a link between two half chains. Panel (b): addition of a small world link. Panel (c): addition of a site, with links to two half chains, and to a remote site with probability  $p$ . One computes the energy shifts associated with these operations as a function of the fields  $g_i$  and  $h_i$ .

(Fig. 8b) and  $\Delta E_1$  when adding a site (Fig. 8c). The energy is then given by the formula:

$$E = \Delta E_1 - \Delta E_2^C - \frac{1}{2} \Delta E_2^{SW} . \tag{5}$$

Along the floppy branch of solution,  $E$  is simply given by the expression  $E = 1 - (5/2)p$ . The transition takes place when the energy of the rigid solution crosses this straight line, for  $p_c \simeq 0.368$ , see Fig. 9. The agreement with the numerical results is excellent.

The size of the largest rigid and stressed clusters can also be calculated following ref. 8. Analytical and numerical results are again in perfect agreement, except close to the transition, where the discrepancy is probably due to finite size effects, see Fig. 10.

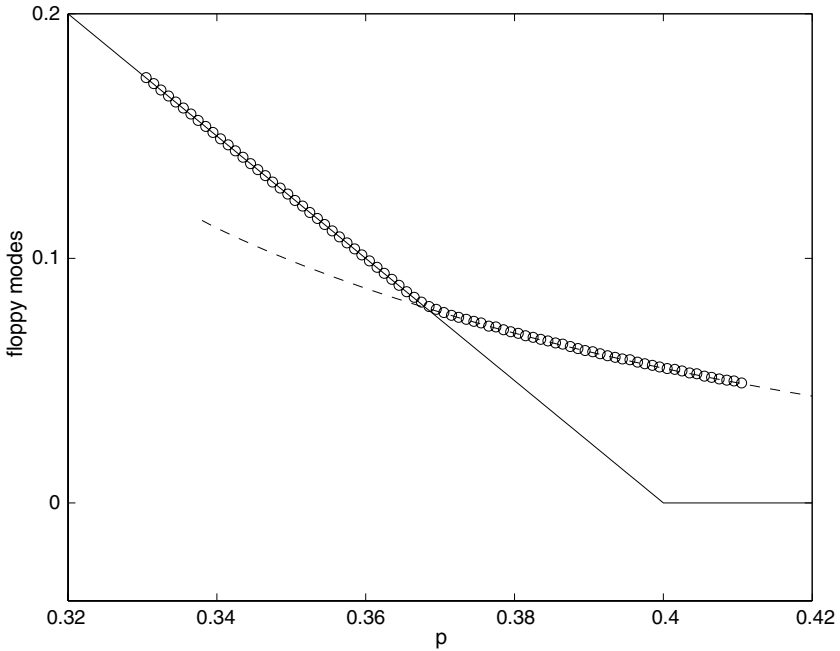


Fig. 9. Number of floppy modes per site as a function of  $p$  for the small world chain. The solid straight line is the low  $p$  solution; the dashed line is the non-trivial solution. The circles are results of numerical calculations using the pebble game algorithm,<sup>(14)</sup> on graphs of 20,000 sites, each data point being averaged over 100–300 graph realizations.

## 5. DISCUSSION

Developing the analogy between rigidity theory and combinatorial optimization facilitates the use of similar ideas in both fields, and provides a means of examining a number of issues from a new point of view. For example, we have shown in this paper that the transfer matrix method introduced previously<sup>(6,8)</sup> is equivalent to the cavity method at the replica-symmetric level. However, it is well known in the context of combinatorial optimization and spin glass theory that the cavity method at the replica-symmetric level gives incorrect results in many instances: it is necessary to introduce the possibility of breaking the replica symmetry. It is thus striking that in all rigidity models studied so far, the transfer matrix or cavity solution seems to be exact: extensive and accurate numerical calculations with the pebble game algorithm show little discrepancy, in 2D or 3D, with bond-stretching constraints only, or with bond-bending as well as bond-stretching constraints. It is reasonable to conjecture that this is true

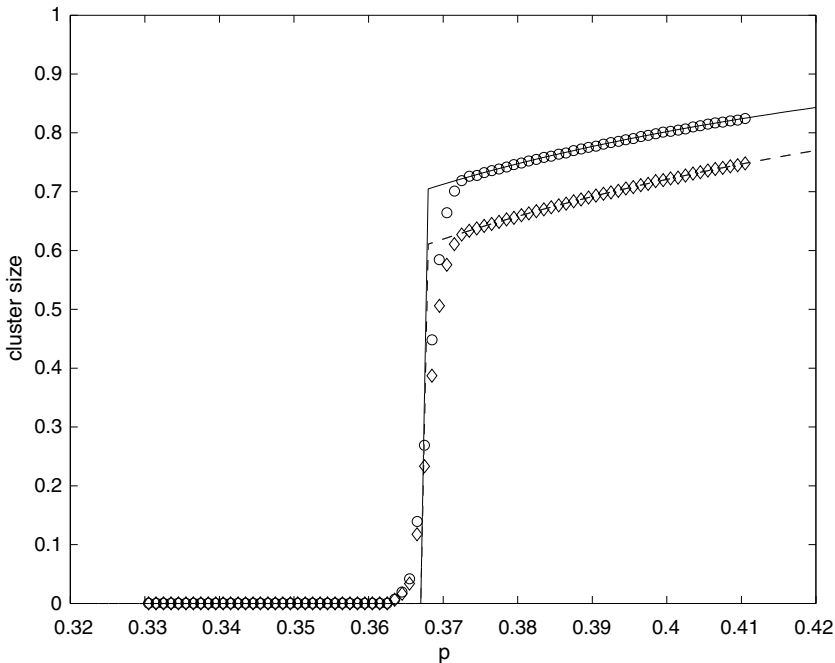


Fig. 10. Analytical calculations and numerical results for the size of the largest rigid cluster (solid line and circles) and the size of the largest stressed cluster (dashed line and diamonds) of the small world chain. As above the numerical calculations are done using the pebble game algorithm, on  $N=20,000$  site graphs, and averaged over 100–300 realizations.

for any rigidity model solvable with the cavity method. Since it is believed that the failure of the replica-symmetric cavity method coincides with the onset of exponential complexity<sup>3</sup> for the corresponding algorithm,<sup>(9)</sup> this conjecture is consistent with the fact that the pebble game algorithm never runs in a time exponential in the number of sites. It was suggested a few years ago that this onset of complexity could be directly related to the order of the phase transition.<sup>(10)</sup> Indeed, 2-SAT undergoes a second order phase transition between a satisfiable and an unsatisfiable phase, shows no replica-symmetry breaking and is never exponentially complex. 3-SAT, as well as  $K$ -SAT for  $K \geq 3$ , undergo a first order phase transition, a replica-symmetry breaking, and are exponentially complex in the vicinity of the phase transition. The randomly bonded rigidity models all display a first order phase transition, no replica-symmetry breaking, and no exponential

<sup>3</sup>That is the algorithm which finds the ground state of the effective Hamiltonian for the problem runs in a time increasing exponentially with the number of sites in the network.

complexity; in this sense, they are a counter-example to the conjecture in ref. 10.

Recently, the concept of an “intermediate phase” as a precursor to the phase transition has emerged independently in both combinatorial optimization<sup>(9)</sup> and in network glasses (both theoretically and experimentally).<sup>(11,12)</sup> It is natural to ask whether these intermediate phases are related. In combinatorial optimization, this phase corresponds to a failure of the replica-symmetric assumption; in networks, it is related to the possibility of self-organization or adaptability of the underlying network.<sup>(12)</sup> Since no replica-symmetry breaking seems to occur in rigidity models, these two types of intermediate phases do not seem to bear a common mathematical description. However, since we have established a precise correspondence between rigidity and some combinatorial problems, one can ask how general is the intermediate phase revealed in network glasses, and if it can be relevant to combinatorial optimization problems. This question is addressed in J. Barré *et al.* (submitted), where it is suggested that an intermediate phase could indeed exist in some combinatorial problems.

## 6. CONCLUSION

In conclusion, we have shown in this paper that the transfer matrix technique used to solve Random Bond Models of the rigidity transition<sup>(8)</sup> is a special case of the general cavity method. This puts on a firm ground the analogy between certain combinatorial optimization problems such as K-SAT and the rigidity transition: their common mathematical structure allows for the use of the same analytical tools. As an example of the versatility of the cavity method, we have studied the rigidity transition of a small world chain; the agreement with numerical studies is perfect, suggesting that the solution is exact for this example.

Developing the analogy and a common language between the two fields should allow a fruitful cross-fertilization for understanding the rich behavior of networks arising in many contexts, including glasses and biology, economic and social sciences.

## ACKNOWLEDGMENTS

We would like to thank Don Jacobs, Mykyta Chubinsky and Michael Thorpe for permission to use the software Pebble-3D. Work at Los Alamos National Laboratory was supported by the U.S. Department of Energy.

## REFERENCES

1. J. C. Phillips, *J. Non-Cryst. Sol.* **34**:153 (1979).
2. M. F. Thorpe, *J. Non-Cryst. Sol.* **57**:355 (1983).
3. W. Bresser, P. Boolchand, and P. Suranyi, *Phys. Rev. Lett.* **56**:2493 (1986).
4. M. F. Thorpe, M. Lei, A. J. Rader, D. J. Jacobs, and L. A. Kuhn, *J. Mol. Graph.* **19**:60 (2001).
5. S. Feng and M. Sahimi, *Phys. Rev. B* **31**:1671 (1985).
6. P. M. Duxbury, D. J. Jacobs, M. F. Thorpe, and C. Moukarzel, *Phys. Rev. E* **59**:2084 (1999).
7. M. F. Thorpe, D. J. Jacobs, N. V. Chubinsky, and A. J. Rader, in *Rigidity Theory and Applications*, M. F. Thorpe and P. M. Duxbury eds. (Kluwer Academic/Plenum Publishers, New York, 1999).
8. N. V. Chubinsky, PhD Thesis, Michigan State University (2003).
9. M. Mézard, G. Parisi, and R. Zecchina, *Science* **297**:812 (2002).
10. R. Monasson, R. Zecchina, S. Kirkpatrick, B. Selman, and L. Troyanski, *Nature* **400**:133 (1999).
11. Y. Wang, P. Boolchand, and M. Micoulaut, *Europhys. Lett.* **52**:633 (2000).
12. M. F. Thorpe, D. J. Jacobs, M. V. Chubinsky, and J. C. Phillips, *J. Non-Cryst. Sol.* **266–269**:859 (2000).
13. G. Laman, *J. Eng. Math.* **4**:331 (1970).
14. D. J. Jacobs and M. F. Thorpe, *Phys. Rev. Lett.* **75**:4051 (1995).
15. C. Moukarzel and P. M. Duxbury, *Phys. Rev. Lett.* **75**:4055 (1995).
16. D. J. Jacobs, *J. Phys. A: Math. Gen.* **31**:6653 (1998).
17. M. Mézard and G. Parisi, *J. Stat. Phys.* **111**:1 (2003).
18. D. J. Watts and S. Strogatz, *Nature* **393**:440 (1998).